

Northumbria Research Link

Citation: Hamylton, Sarah and East, Holly (2012) A Geospatial Appraisal of Ecological and Geomorphic Change on Diego Garcia Atoll, Chagos Islands (British Indian Ocean Territory). Remote Sensing, 4 (11). pp. 3444-3461. ISSN 2072-4292

Published by: MDPI

URL: <http://dx.doi.org/10.3390/rs4113444> <<http://dx.doi.org/10.3390/rs4113444>>

This version was downloaded from Northumbria Research Link:
<http://nrl.northumbria.ac.uk/id/eprint/37260/>

Northumbria University has developed Northumbria Research Link (NRL) to enable users to access the University's research output. Copyright © and moral rights for items on NRL are retained by the individual author(s) and/or other copyright owners. Single copies of full items can be reproduced, displayed or performed, and given to third parties in any format or medium for personal research or study, educational, or not-for-profit purposes without prior permission or charge, provided the authors, title and full bibliographic details are given, as well as a hyperlink and/or URL to the original metadata page. The content must not be changed in any way. Full items must not be sold commercially in any format or medium without formal permission of the copyright holder. The full policy is available online: <http://nrl.northumbria.ac.uk/policies.html>

This document may differ from the final, published version of the research and has been made available online in accordance with publisher policies. To read and/or cite from the published version of the research, please visit the publisher's website (a subscription may be required.)



**Northumbria
University**
NEWCASTLE



UniversityLibrary

Article

A Geospatial Appraisal of Ecological and Geomorphic Change on Diego Garcia Atoll, Chagos Islands (British Indian Ocean Territory)

Sarah Hamylton ^{1,*} and Holly East ²

¹ School of Earth and Environmental Sciences, University of Wollongong, Wollongong, NSW 2522, Australia

² Department of Geography, University of Cambridge, Tennis Court Road, Cambridge CB2 3EN, UK; E-Mail: hke21@hermes.cam.ac.uk

* Author to whom correspondence should be addressed; E-Mail: shamylto@uow.edu.au; Tel.: +61-02-4221-3589; Fax: +61-02-4221-4250.

Received: 31 August 2012; in revised form: 15 October 2012 / Accepted: 25 October 2012 /

Published: 12 November 2012

Abstract: This study compiled a wide range of modern and historic geospatial datasets to examine ecological and geomorphic change at Diego Garcia Atoll across a 38-year period (1967–2005). This remarkable collection of spatially referenced information offered an opportunity to advance our understanding of the nature and extent of environmental change that has taken place with the construction of the military airbase at Diego Garcia. Changes assessed included movements of the lagoon rim shorelines, changes in the terrestrial vegetation on the lagoon rim and amendments to the bathymetry of the lagoon basin through dredging activities. Data compiled included detailed shoreline and vegetation maps produced as part of the H.M.S. Vidal Indian Ocean Expedition (1967), three Ikonos satellite images acquired in 2005 that collectively covered the complete Atoll area, a ground truthing field dataset collected in the northern section of the lagoon for the purpose of seafloor mapping (2005), observational evidence of shoreline erosion including photographs and descriptions of seawater inundations and bathymetric soundings from five independent surveys of the lagoon floor (1967, 1985, 1987, 1988 and 1997). Results indicated that much of the change along the lagoon rim is associated with the expansion of the inner lagoon shoreline as a result of the construction of the military airbase, with an estimated increase in land area of 3.01 km² in this portion of the atoll rim. Comparisons of 69 rim width transects measured from 1967 and 2005 indicated that shorelines are both eroding (26 transects) and accreting (43 transects). Within a total vegetated area of 24 km²,

there was a notable transition from Cocos Woodland to Broadleaf Woodland for a land area of 5.6 km². From the hydrographic surveys, it was estimated that approximately 0.55 km³ of carbonate sediment material has been removed from the northwest quadrant of the lagoon, particularly in the vicinity of the Main Passage. As no previous record of benthic character exists, a complete benthic habitat map of the atoll was derived through classification of the three IKONOS satellite images. Management implications arising from this overall appraisal of geomorphic and ecological change at Diego Garcia included the need for ongoing monitoring of shoreline change at a representative set of sites around the atoll rim, monitoring of the water flow regime through the northern channels between the open ocean and the lagoon basin and an ongoing mapping campaign to record periodic changes in the character of the benthic surface ecology.

Keywords: Chagos Islands; shoreline; change detection; benthic habitat

1. Introduction

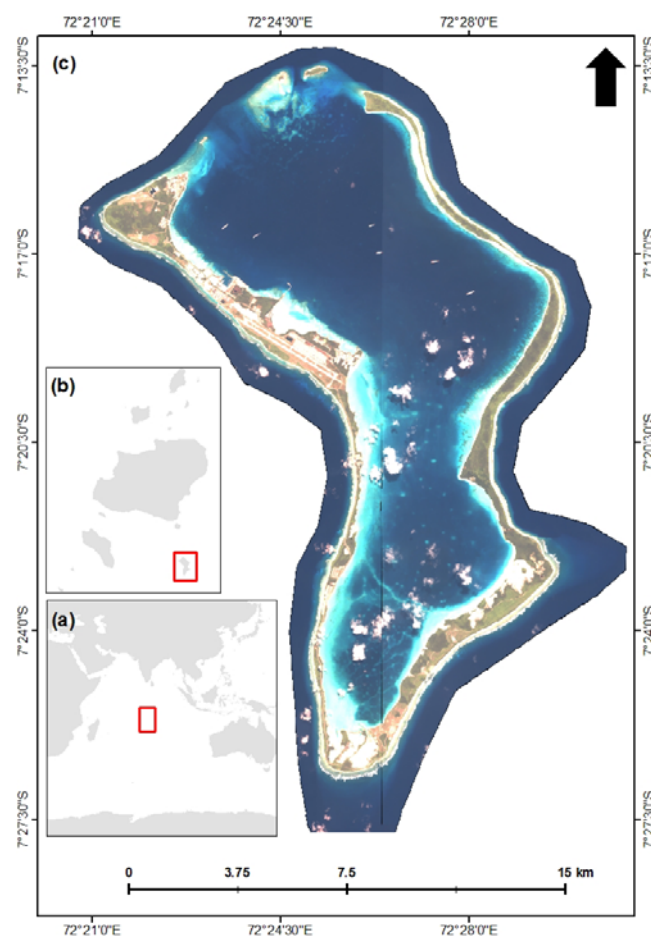
The Chagos Archipelago is a group of 55 isolated, low-lying coral islands in the central Indian Ocean located between Longitude 71–73°E and Latitude 4.5–7.5°S (Figure 1). They are supported by the submerged Chagos banks at the southern end of a linear array of islands that include the Maldives and Laccadives. The islands and their associated reefs are thought to be in pristine condition due to the absence of environmental pressures such as fishing, tourism, terrigenous sedimentation and pollution [1]. They support a wealth of marine biodiversity including live coral, reef fishes, coconut crab, turtle and bird colonies [1]. The archipelago was designated the world's largest no-take marine protected area in 2010 (>550,000 km²). Within the context of the wider Indian Ocean region, the reefs of the Chagos islands are functionally important as they provide a geographical and genetic linkage between the West Indian Ocean and Indo-Pacific biogeographic provinces. This permits the movement of marine species such as coral larvae along the south equatorial current towards the Seychelles in the west and along the south equatorial counter-current towards Thailand and Cocos-Keeling in the east [2]. Strong linkages exist between the ecological and geomorphic processes occurring across the Chagos reef platforms and observable changes in their structure over time. These suggest that an assessment of the magnitude and location of change would be a profitable exercise to inform coastal and marine management at this regionally significant site.

The archipelago consists of a wide range of reef island types (atolls, vegetated and unvegetated sand cays). These islands are subject to a combination of regional oceanographic factors including the Indian Ocean Dipole, reversing annual monsoons, the Southern Equatorial Current and seasonal Tropical Cyclones [3]. For approximately eight months of the year the prevailing winds blow from the southeast, with remaining seasons fluctuating between westerly winds and transitional conditions [12]. This regime is reflected in the local wave climate and the islands therefore have a natural history of geomorphic mobility due to seasonal shifts in sediment supply, storm and wave activity.

Indian Ocean reef platforms and the islands they support have stabilized in their current configuration as Holocene sea levels have slowly risen over the past 6000 years [4–6]. However, their

response to more recent climatic changes such as accelerated sea level rise, coral bleaching and increased intensity of storms has shown great variability across different localities. While the absence of a continuous monitoring program precludes a robust analysis at one particular site, islands within the wider Chagos region show variable change over the last 230 years. This includes the apparent submergence of three sandy islets previously observed at Blenheim atoll in the north [7] and island growth and fusion of six sandy islets at Egmont Atoll [1]. Regional sea surface temperature increases have reduced live coral cover through bleaching across several of the reef platforms, most notably the 1998 warming event associated with the El Nino Southern Oscillation [8]. Coral recovery has subsequently been observed and from a geomorphic perspective, this event would have resulted in short term accretion through a pulse of detrital carbonate sediment supply. However, longer term reductions in available carbonate sediment supply may have contributed to shoreline retreat evident in some locations in the form of erosion ramps and cliffed beaches [12]. The population of Chagos was relocated in the 1970s, after which Diego Garcia became an American air base, thus, more recent anthropogenic influences associated with the construction of military infrastructure have been superimposed onto existing atoll dynamics.

Figure 1. The study site (a) the location of the British Indian Ocean Territory in the central Indian Ocean, (b) the location of Diego Garcia at the southern end of the Chagos archipelago (BIOT), and (c) Diego Garcia atoll.



Advances in the collection of geospatial data, particularly in the development and application of remote sensing technology to reef systems [10,11] afford an opportunity for monitoring change in both reef platforms and the islands they support at decadal timescales. Significantly for the Diego Garcia site, several comprehensive historical geospatial datasets exist which can be treated as a baseline against which change can be assessed. As such datasets do not appear to be available for comparable atoll sites of military development (e.g., in the Pacific). This therefore represents the first geospatial assessment of ecological and geomorphological change associated with this coastal land use practice. The objective of this study is to compile a wide range of modern and historic geospatial datasets for the examination of both ecological and geomorphic change at Diego Garcia Atoll. Data compiled include detailed shoreline and vegetation maps produced as part of the 1967 H.M.S. Vidal Indian Ocean Expedition [12], three recent Ikonos satellite images acquired in 2005 that collectively cover the complete Atoll area and bathymetric soundings from five independent surveys of the lagoon floor (1967, 1985, 1987, 1988 and 1997) (see Table 1). Change is investigated across three atoll sub-environments, including movements of the lagoon rim shorelines, changes in the terrestrial vegetation on the lagoon rim, and amendments to the bathymetry of the lagoon basin, primarily through dredging activities, across a 38-year period (1967–2005). In the absence of available baseline information, a map of the atoll benthic character is also provided as a record against which future change can be measured.

Table 1. A summary of the raw and derived datasets compiled for the assessment of ecological and geomorphic change on Diego Garcia.

	<i>Dataset</i>	<i>Source</i>	<i>Resolution</i>
Raw dataset	1971 Shoreline map (1971)	Atoll Research Bulletin (Stoddart, 1971)	0.75 m
	Vegetation map (1971)	Atoll Research Bulletin (Stoddart, 1971)	0.75 m
	Ikonos satellite images (2005)	GeoEye Foundation	3.2 m
	Hydrographic charts (1967, 1985, 1987, 1988 and 1997)	UK Hydrographic Office, United States Geological Survey	5 m
Derived dataset	Shoreline position (denoted by vegetation edge) (2005)	Digitized at a scale of 1:1500 from Ikonos satellite images	0.75 m
	Vegetation map (2005)	Derived from an unsupervised classification of the IKONOS satellite images	3.2 m
	Lagoon bathymetric model	Derived from a kriging interpolation of the 2590 bathymetric soundings	25 m
	Benthic cover map (2005)	Derived from an unsupervised classification of Ikonos satellite images	3.2 m

1.2. Study Area

Diego Garcia is a horse-shoe shaped atoll ($9 \times 22 \text{ km}^2$) that lies 55 km south of the Great Chagos Bank and represents over half the land area of the 55 archipelago islands. Approximately 70% of the atoll area is comprised of the extensive lagoon (11 km^2), which is enclosed by one of the most continuous land rims of all coral atolls [13]. Isolated dunes rise to 9 m above sea level, although more commonly they reach around 5 m height on shores that are exposed to southwesterly winds [12]. Spring tidal ranges reach approximately 1.6 m and the carbonate limestone land rim has a freshwater lens that is sustained by the highest levels of rainfall in the Indian Ocean [12]. This has enabled the

land rim, which is approximately 57 km in length and over 2 km wide in places, to support a well-developed vegetation community. Coconut plantations dominated the island vegetation community while the atoll was under English and French colonial control between 1876 and 1971. These were extensively cleared along the western atoll rim and several invasive species were added during construction of the airbase, beginning in 1971. Native vegetation remains in other parts of the island and in places this has transitioned through several successional stages including coastal grasses and sedges, littoral scrubs and hedges (e.g., *Scaevola taccada*), a mixture of shrubs and juvenile trees, termed locally as “Cocos Bon-Dieu”, broadleaf woodland and planted coconut trees [13].

The lagoon reaches a depth of 31 m in the center and can be broadly divided into three basins running from north to south that get progressively shallower and host more intricate topography, including coral knolls and limestone ridges. Around the external atoll periphery, the bathymetric profile of the forereef slopes steeply down to depths of 400 m within a short distance of the exposed atoll rim (<1 km).

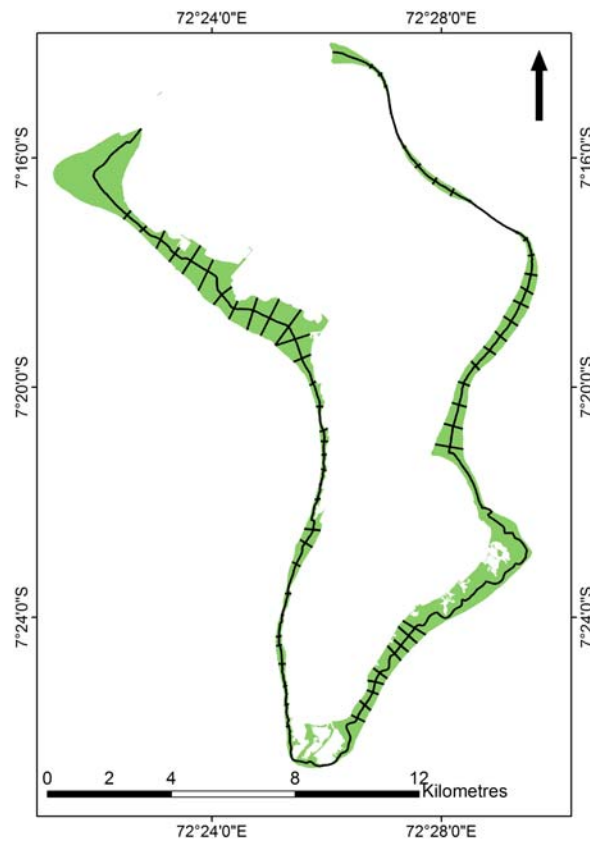
2. Methods

2.1. Lagoon Rim Shoreline Change

A map produced from a 1967 survey of atoll vegetation [12] was scanned and georeferenced according to the coordinate gridlines provided. This was then digitized in ArcMap 10 at a scale of 1:1,500 to produce a digital vector record of the early vegetation edge. As a measure of the corresponding 2005 shoreline position, the vegetation boundary of the 2005 IKONOS images was digitized in the same manner. The vegetation edge was used as a proxy for shoreline position to eliminate any uncertainty associated with seasonal and tidal fluctuations that may influence determination of the shoreline edge [14,15].

To compare the two shoreline datasets, a polyline file was created that comprised 69 rim width transects running perpendicular to the shoreline around the atoll boundary (Figure 2). For each transect the difference between the length on the 1967 shoreline and the 2005 shoreline was measured to produce a record of the magnitude of shoreline change during the intervening period. To estimate the error associated with this procedure, a similar approach was adopted to that used by Ford (2012) for estimating shoreline changes on Majuro Atoll. Error was quantified as the square root of the sum of the constituent errors squared, where constituent errors were comprised of the digitizing and pixel error. Digitizing error was calculated as the standard deviation in shoreline positions from repeated digitization of the same section of coast at a scale of 1:1500 and the pixel error related to the spatial resolution of the images used (see Table 1). By way of additional validation, change measurements were compared to a georeferenced collection of 8 photorecords of shoreline change between 2009 and 2012 [16].

To assess whether there were significant differences in the extent of shoreline change between the “narrow” and “normal” rim types [12], an analysis of covariance (ANCOVA) test was applied to the rim width transect change records. This controlled for the influence anthropogenic activity as a potential covariate. The proportion of human influence on each width transect was measured as the length of transect intersected by infrastructure and used as a metric for anthropogenic activity.

Figure 2. Location of shoreline transects around the Atoll rim.

2.2. Lagoon Rim Vegetation Change

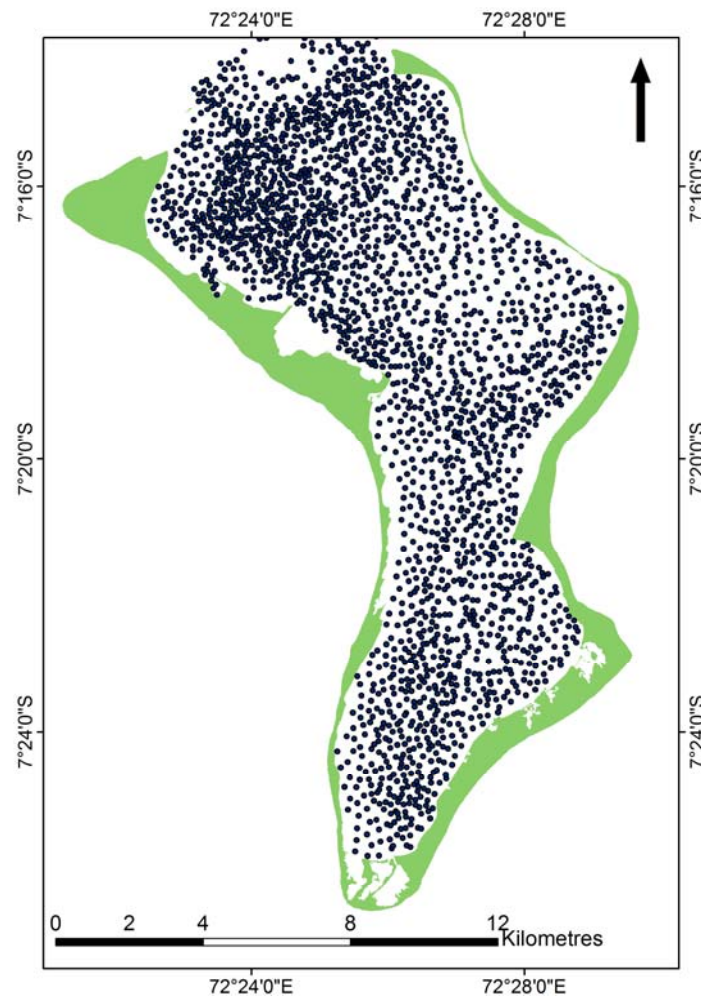
Changes in the nature and spatial distribution of vegetation communities around the atoll rim were assessed against a vegetation map that was previously constructed in 1967 [12]. The map, comprised of 10 vegetation classes, was scanned, georeferenced and digitized prior to comparison against an updated terrestrial vegetation map produced by classifying the component wavebands of the 2005 Ikonos satellite imagery. An unsupervised maximum likelihood classification was performed in Erdas Imagine to assign pixels to the most likely class [17]. Although no terrestrial ground truth data exists for Diego Garcia to assist validation of the output map, confidence may be gained from the fact that spectral differences corresponded with boundaries between classes in the earlier map. To assess in detail the differences between these two maps, a change matrix was constructed [18]. Classes were coded using successive powers of two to ensure every possible land cover transition could be identified by a unique value and the 2005 and 1967 digital map files were then differenced to generate the change matrix.

2.3. Lagoon Bathymetric Change

Bathymetric change within the lagoon basin was assessed using detailed sounding charts developed from hydrographic surveys in 1967 (H.M.S. Vidal) and 1998 (UK Hydrographic Office). The sounding density of the 1967 survey ranged from 100 to 200 depth records per km², the third highest density of any atoll surveys undertaken prior to 1970, following Addu and Eniwetok [12]. The 1998 chart compiled subsequent soundings from two US government surveys of 1987 and 1988, and a further

British Admiralty survey in 1997. Surveys undertaken after 1967 focused primarily in the northern sector of the lagoon adjacent to the military base, an area that has been extensively dredged. A total of 2590 numbered points from each sounding chart within the lagoon were digitized into a point file (Figure 3). These were subsequently spatially interpolated using a kriging algorithm to generate a continuous bathymetric model covering the complete lagoon area. An additional 994 points were then digitized from the subsequent hydrographic surveys to produce an updated bathymetric lagoon model and the two surfaces were then differenced to produce a bathymetric change model.

Figure 3. Point file displaying the 3,584 soundings from the 1998 UK Hydrographic Office bathymetric chart.



It was possible to calculate the net change in volume of sediment throughout the appraisal time period by summing across the raster pixels that comprised the bathymetric change model and subtracting those that represented sediment loss from sediment accumulation (Equation (1)).

$$\Delta VSed = \sum VSed_{ac} - VSed_{rem} \quad (1)$$

where $\Delta VSed$ = Net change in sediment volume,

$VSed_{ac}$ = Total volume of sediment accumulated,

$VSed_{rem}$ = Total volume of sediment removed.

2.4. Construction of a Benthic Cover Map

Three separate IKONOS satellite images were acquired for the site on 7 May, 28 May and 18 June 2005. These were largely free of cloud cover and sun glint at the water surface, affording a clear view of the seafloor around the atoll. IKONOS imagery was pre-processed to correct for the effects of scattering and absorption in the atmosphere and water column. Water column correction followed a methodology that assumed that the vertical radiative transfer through a water column could be approximated to a logarithmic decrease in radiation with depth [19]. Individual waveband data were log transformed and regressed against each other to calculate a depth invariant index for each band pair. This was calculated for multiple waveband pairs to generate a series of depth invariant bands upon which a statistical image classification could be performed [20]. To map the benthic habitat of the atoll, a maximum likelihood classification was performed in Erdas Imagine on the depth invariant bands, which assigned pixels to the most likely class [17]. An independent ground truthing dataset composed of 250 records of benthic community composition was used to calibrate and conduct an accuracy assessment of the classification [21]. Of the ground truthing points, 119 were used to train the classifier and 131 were used to validate the classification output. Overall accuracy was quantified by dividing the number of pixels correctly identified by the total number of pixels in the validation [22].

3. Results

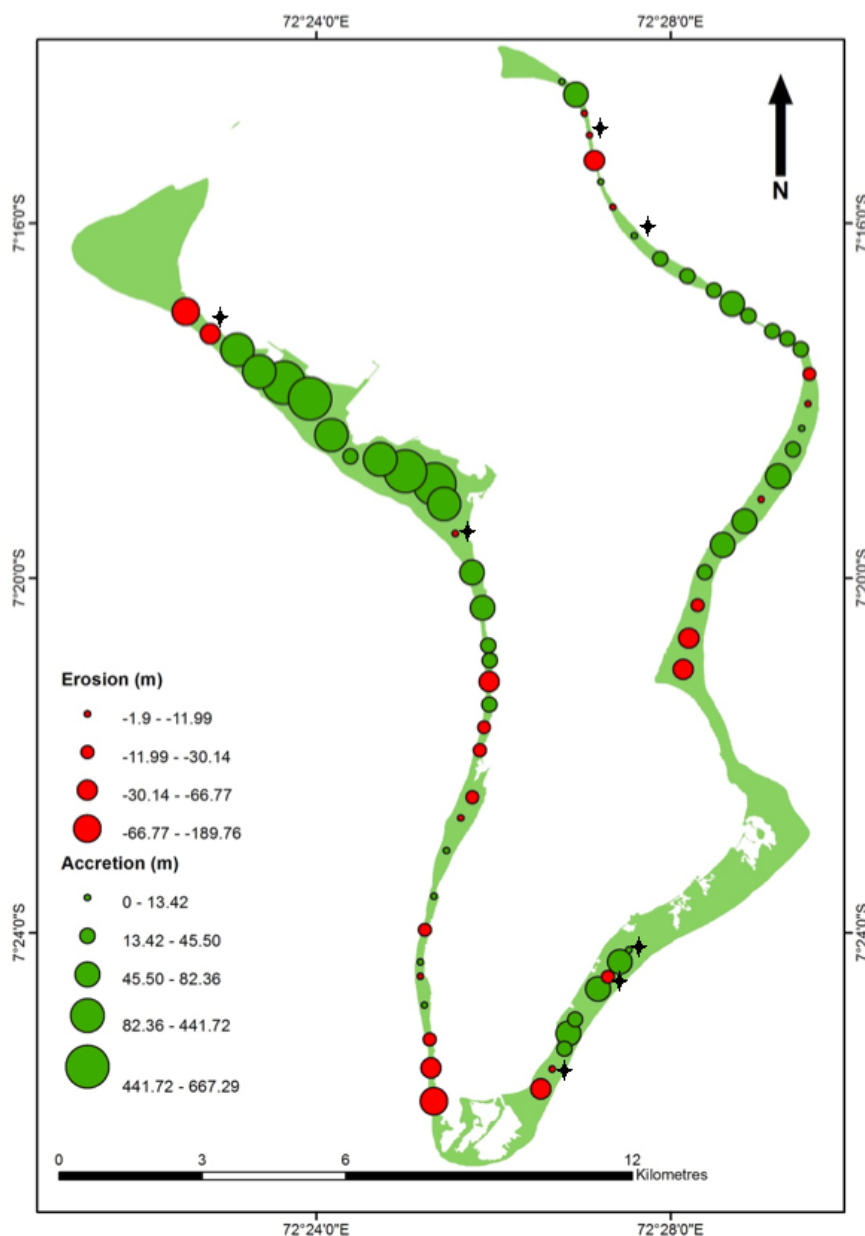
3.1. Lagoon Rim Shoreline Change

Measurements from the rim width transects indicated that the atoll shorelines were both eroding and accreting (Figure 4). Of the 69 rim width transects assessed, 26 were estimated to have eroded over the assessment time period and 43 were estimated to have accreted. The majority of the accretion occurred in association with the development of the military base along the northwestern section of the atoll rim and along the straighter rim segments on the eastern coast. Total quantifiable error for this assessment was estimated at ± 4.54 m, which meant that of the 69 rim width transects, the magnitude of change detected across seven of these transects did not exceed the error range associated with the methodology employed (Figure 4), however, for the remaining 60 transects, the change fell outside this range and therefore appeared to be significant.

The most substantial change detected was associated with build-out of the lagoon rim in the northwest for the air base. A statistically significant difference was found to exist between the collective measurements taken from the different “narrow” vs. “normal” rim types identified [12] (ANCOVA, $F_{1,66} = 7.382$, $P = 0.008$).

Of the 8 independent photorecords employed as validation [16], the four exhibiting erosion were also associated with erosion in analysis of rim width transects. The remaining four photorecords suggested no shoreline change, but measurements in the present study suggested that rim widths had eroded over the longer 38-year period.

Figure 4. Change in rim width (m) between Stoddart's 1967 survey & the 2005 IKONOS images. Black crosses denote points where the estimated change fell within the methodological error range.



3.2. Lagoon rim Vegetation Change

Figure 5 illustrates the vegetation communities mapped around the atoll rim from the detailed air photography in 1967 and through classification of the Ikonos satellite imagery in 2005, while Table 2 details the change matrix generated from these maps.

The vegetation matrix (Table 2) indicated that the greatest change was the reduction of Cocos Bon-Dieu from 12.41 km² in 1967 to 3.88 km² in 2005, 5.63 km² of which became Broadleaf Woodland. This vegetation category substantially increased from 2.90 km² in 1967 to 9.11 km² in 2005.

Figure 5. Atoll vegetation in 1967 (Stoddart, 1971) and 2005 derived from the IKONOS satellite images.

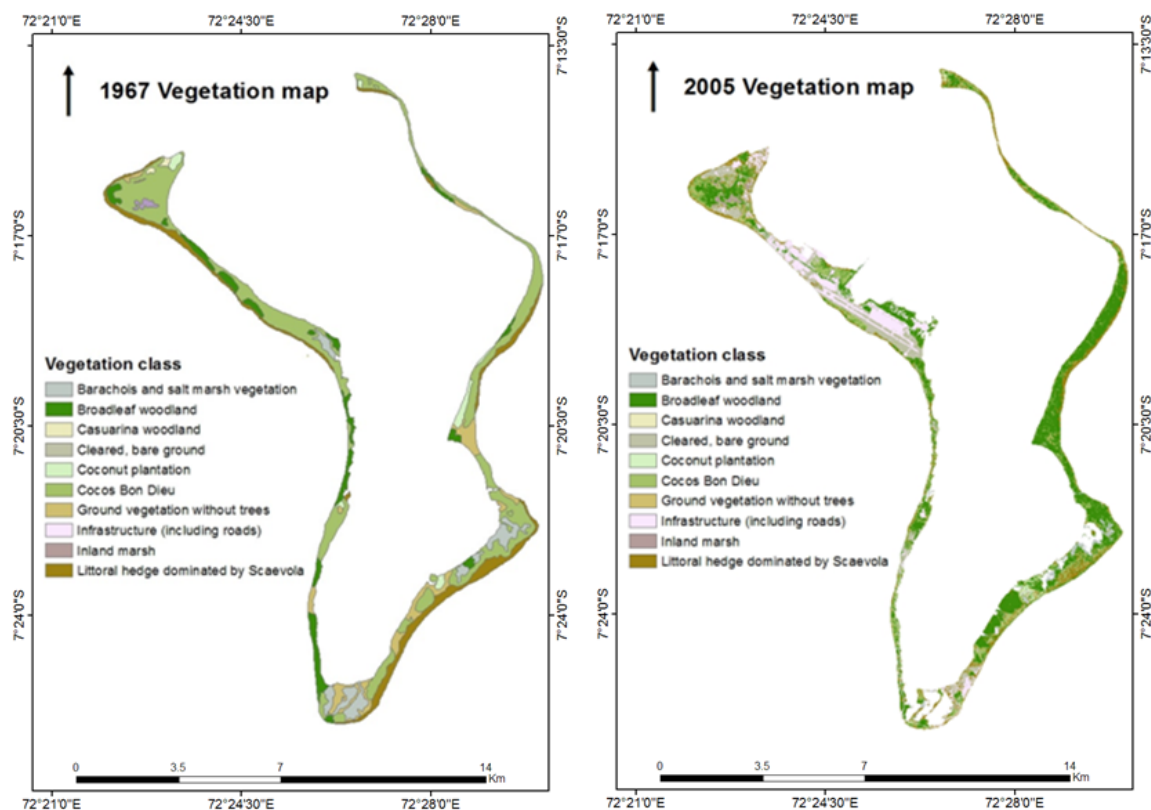


Table 2. A change detection matrix generated from comparing the areas of classes mapped in 1967 and 2005 vegetation maps. Numbers indicate the difference in area mapped for each vegetation category, bold numbers along the diagonal indicate areas mapped consistently (units are in km², cumulative error ± 17.6 m²).

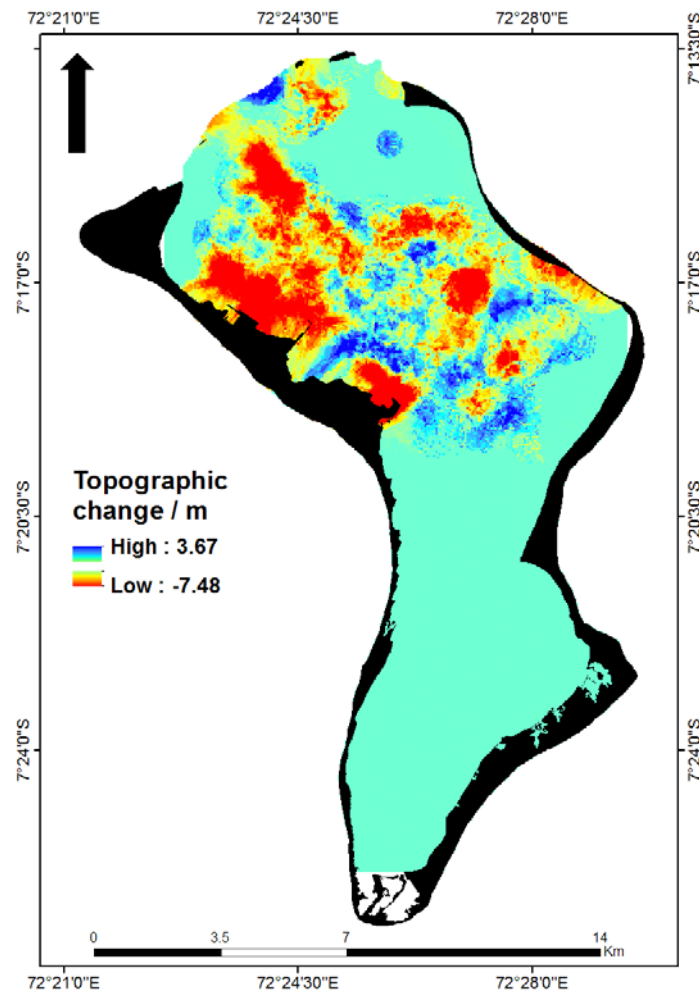
	1967							Total 2005:
	Broadleaf Woodland	Cocos Bon-Dieu	Littoral Hedge	Ground Vegetation	Coconut Plantation	Inland Marsh	Casuarina Woodland	
2005								
Broadleaf Woodland	0.93	5.63	0.91	1.18	0.38	0.07	0.02	9.11
Cocos Bon-Dieu	0.74	1.80	0.82	0.41	0.06	0.04	0.00	3.88
Littoral Hedge	0.31	1.26	1.30	0.24	0.06	0.00	0.02	3.19
Ground Vegetation	0.04	0.17	0.23	0.05	0.01	0.00	0.00	0.51
Coconut Plantation	0.00	0.09	0.09	0.07	0.09	0.00	0.00	0.34
Inland Marsh	0.34	1.09	0.16	0.00	0.00	0.07	0.00	1.66
Infrastructure	0.21	0.63	0.29	0.12	0.10	0.00	0.07	1.41
Cleared/Bare Ground	0.33	1.75	0.46	0.13	0.06	0.00	0.02	2.75
Total 1967:	2.90	12.41	4.26	2.21	0.76	0.18	0.13	

3.3. Lagoon Bathymetric Change

Figure 6 shows the bathymetric change modeled for the northern sector of the lagoon for the period 1967–1998. The total volume of the lagoon was found to be 1.31 km³ in 1967 and 1.86 km³ in 1998,

indicating a net volume of sediment removal of 0.55 km^3 from the lagoon (cumulative error $\pm 0.000625 \text{ km}^3$). The majority of sediment removal (depicted in red) was associated with the dredging for the military airbase in the northwestern sector of the lagoon, while some was also evident in the channels connecting the lagoon basin to the open ocean in the north, particularly in Main Passage.

Figure 6. A model of bathymetric change (m) within the lagoon, produced by subtracting the UK hydrographic survey data (1998) from that collected by the H.M.S. Vidal survey (1967). Red indicates sediment removal, blue indicates accretion and turquoise indicates no change.



3.4. The Benthic Cover Map

To the best of the authors' knowledge, Figure 7 represents the first detailed record of benthic cover around Diego Garcia Atoll. Table 3 provides a description for each benthic cover type mapped. An overall accuracy of 70% was achieved when this was compared against an independent dataset of 131 ground referencing points. The classification was dominated by the deep (46%) and shallow (19%) lagoon floor classes, followed by reef flat (14%) and lagoonal slope (12%). The reef flat was characterized by coral sand and rubble at shallow water depths (<2 m), with frequent pools and *Porites lutea* bommie fields [21]. The lagoonal slope class comprised live coral cover of between 70 and 100%, dominated by *Acropora tenuis* [21].

Figure 7. Benthic cover map generated from Ikonos imagery and Purkis *et al.*'s [21] ground truth data. The pie chart illustrates the relative proportions of each cover type mapped by the classification.

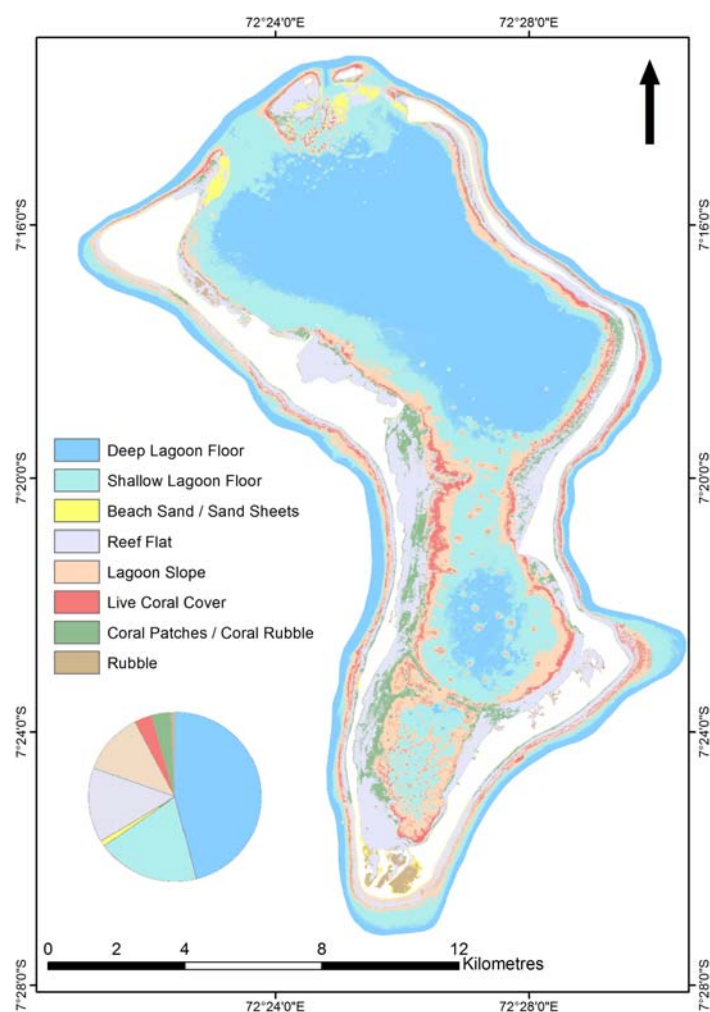


Table 3. Description of each of the benthic cover classes mapped.

Class	Description
Deep lagoon floor	Carbonate lagoon sediments with poor sorting and a wide range of mean particle sizes (low coral cover <2%). Intermittent coral knolls at depths of −15 m to −18 m. Depths typically < −15 m.
Shallow lagoon floor	Size and sediment characteristics akin to those of lagoon beaches. Depths between c. −6 m and −15 m. The small circular areas of shallow lagoon floor surrounded by the deep lagoon floor class (e.g., in the lagoon entrance) represent knolls.
Beach sand/Sand sheets	Unvegetated carbonate sediments and rubble.
reef flat	Bare rock, algal communities, coralline sand and rubble at shallow (<2 m) depths with frequent pools and <i>Porites lutea</i> bommie fields.
Lagoon slope	Live coral cover (70–100%), dominated by <i>Acropora tenuis</i> .
Live coral cover	High live coral cover (80–100%) including a high proportion of wave resistant coral taxa outside of the lagoon and on knoll rims.
Coral patches/coral rubble	Coralline rubble and small bommies, typically on the reef flat.

4. Discussion

Some degree of natural variability in shoreline position around the atoll rim is to be expected as reef islands are by nature unconsolidated sedimentary landforms, the deposition of which is strongly controlled by waves [23]. This variability is apparent around the rim of Diego Garcia, with 43 points indicating net accretion and 26 points indicating net erosion across the appraisal period. It is difficult to compare these findings to shoreline change elsewhere as these vary greatly across different localities. For example, topographic and radiocarbon evidence indicates net accretion rather than erosion of oceanward atoll island shores at Cocos-Keeling, Kiribati, Funafuti and the Maldives [24], whereas reduced shoreline protection from coral mortality, has been observed to erode beaches on West Indian Ocean continental islands in the Seychelles [9].

Interpretation of shoreline change around the lagoon rim is aided by the distinction between “narrow” and “normal” atoll rim types [12]. Narrow rims (45–250 m wide) represent geomorphologically recent and unstable links between older land areas that are often subject to along shore sediment transport and common breaching. Normal rims (average width 500 m) are formed by gradual accretion of the seaward beaches, with occasional washovers of sand raising the inland rim surface. These represent some of the oldest and most stable land portions of the atoll rim. The statistically significant difference in the collective change measurements taken from these different rim segments could indicate distinct localized sedimentary dynamics. Such differences with variation around aspects of the atoll rim are evident at other oceanic atolls, for example, Alphonse Atoll in the West Indian Ocean [25] and are likely linked to regional hydrodynamic regimes. The northeastern narrow rim section shows evidence of alongshore sediment transfer, with sediments moving in a southerly direction along the narrow section of the eastern side of the atoll to accumulate on the northern side of Cust Point (Figure 4).

Observations of both erosion and inundation have been recorded elsewhere around Diego Garcia [1,12,16], which accord with evidence of retreat in the form of seaward and lagoonward erosion ramps and cliffing. The degree to which these represent a recent, climate change-driven departure from a longer-term accretion regime, is unclear. In a study of five Indo-Pacific atoll islands including Diego Garcia, Woodroffe suggests that long-term accretion is likely to outweigh short-term observable erosion on atoll rim islands [24]. Lines of evidence for oceanward beaches acting as net sediment sinks include radiocarbon chronologies indicating incremental accretion, the unidirectional progression of waves that transport reef crest sediment across reef flats and multitemporal image and photographic analysis indicating shoreline progradation elsewhere [24]. Radiocarbon chronological sequences have indicated accretion at Cocos-Keeling, a similarly horseshoe-shaped atoll in the East Indian Ocean [26].

The vegetation maps reveal a zonally distributed vegetation mosaic that appears primarily to be controlled by human interference, particularly around the settlement areas. Detailed qualitative descriptions of the 1967 vegetation structure and distribution are available for several subregions of the atoll rim, including Northeast Point, Cust Point, Minni Minni to East Point, East Point to Barachois Maurice, Southeast Rim and the southern, central and northern sectors of the West rim [12]. A subsequent 1997 atoll-wide survey compared the western and eastern sectors of the atoll rim and distinguished the western sector as being comprised of managed land vegetation characterized by a high proportion of invasive alien plant species, landscaped trees and plants of aesthetic value [13]. It is

this area in which most of the vegetation change has occurred (Figure 5). In contrast, the mixed forests of the eastern sector retained a highly diverse proportion of native canopy trees including *Calophyllum*, *Hernandia*, *Cocos* and *Guettarda* [13]. It is difficult to discern the extent to which the apparent vegetation transitions indicated by the change matrix (Table 2) have arisen because of methodological differences in the vegetation mapping procedures employed as opposed to being attributable to real change in vegetation communities. It is clear from the two maps that the satellite classification identified a greater degree of spatial heterogeneity within the vegetation canopy. For example, where a large homogenous patch of Cocos Bon-Dieu was mapped from the aerial photographs in the wide north western extent of the atoll, this same area was subdivided in the satellite classification into Cocos Bon-Dieu, broadleaf woodland, inland marsh, infrastructure and *Scaevola* hedge. While some of this change may be attributable to either clearing of this area associated with the military airbase or a biological succession through vegetation types over the time period of observation, this testifies to the ability of satellite remote sensing approaches to map higher frequency spatial variability in vegetation canopy characteristics. This ability arises because of the increased spectral detail available from the multiple image wavebands and it represents a notable improvement on previous vegetation maps derived from air photos, which are unavoidably generalized [12].

The configuration of lagoon changes indicated by the bathymetric change model results largely from developments associated with the airbase in the northwestern sector of the lagoon. These include artificial shoreline construction, the provision of a turning area for ships and an associated access channel that has been dredged to a depth of 13.6 m leading from the northern channels across to the pier [27]. Topographic highs associated with sediment addition (depicted in blue) are evident around the periphery of the sediment removal sites, possibly as a result of dumping next to excavation sites during dredging activities. The implications of these changes relate primarily to their potential impact on patterns of water circulation across the lagoon basins. It has previously been observed that water exchange between the lagoon and ocean environment is limited [12]. Widening of the lagoon channels is likely to increase the volume of water exchange into and out of the lagoon during each tidal cycle. In turn, this may influence the benthic ecology of the lagoon floor, which is known to be strongly influenced by hydrodynamics in lagoons elsewhere in the Indian Ocean [28], or result in sediment loss to the open ocean.

The collective assessments of change presented in Sections 3.1–3.3 can be more broadly contextualized in relation to other atolls that are sites of military airbases, such as Johnston Atoll (central Pacific) and several sites in the Marshall Islands (South Pacific), notably Enewetak. The magnitude of the ecological and geomorphic change recorded here for Diego Garcia is less dramatic than that recorded at these sites. For example, where infrastructure development has occurred at both these Pacific sites, the islands were stripped of all native vegetation and more extensive areas of the reef platform were dredged. At Johnson atoll this included removal of 700 acres (2.83 km²) of reef structure and sediments, with a detrimental impact on more than 8000 acres (32 km²) of benthic communities [29]. This area is comparable to that dredged at Diego Garcia; however, surveys conducted at Johnston Atoll record much greater ecological impacts. These include reductions in lagoon coral (up to 40% loss of live cover) and other impacts on benthic echinoderms and associated fish biota because of dredging activities and enhanced siltation and water turbidity [29]. Similarly, a series of nuclear weapons tests at Enewetak across the late 1940s and 50s has caused substantial

geomorphic change to the island structure in the form of blast craters (approximately 40 m deep and 1,700 m² in area) that were subsequently used to dispose of contaminated nuclear waste and filled in with concrete [30]. Fallout from these blasts has contaminated the marine environment with radionuclides, which have been detected in lagoon sediments and reef and pelagic fish [31].

To the best of the authors' knowledge, Figure 7 represents the first synoptic, landscape scale record detailing benthic cover around the Atoll. The varying morphological form of the coral patches across the three lagoon basins is evident. While the coral largely exists in the form of isolated knolls in the northern and central lagoon basins, it takes the form of linear networks of ridges to the south. These features have formed from a combination of varying localized water circulation patterns and karst-eroded limestone remnants formed during a period of lower sea level [12]. Although it is likely that coral populations within the lagoon suffered direct damage and silting as a result of construction activities, these have had limited effects on coral populations in the north western quadrant of the northern basin [27]. This is evident in the cover of live coral and lagoonal slope classes mapped, both elsewhere in the northern basin and in other regions of the atoll.

5. Conclusions

Ecological and geomorphic changes recorded for Diego Garcia in this appraisal can be summarized as:

1. Variable levels of shoreline change around different sections of the atoll rim, with measures of both erosion and accretion in accordance observational evidence (ranging from −189.6 m erosion to +667.3 m accretion). Statistically significant differences were detected between apparent change on narrow and normal rim segments, perhaps indicating distinct local geomorphic processes driving shoreline dynamics (ANCOVA, $F_{1,66} = 7.382$, $P = 0.008$).
2. A comparison of vegetation communities mapped in 1967 and 2005 suggests greater recent coverage of broadleaf woodland areas (an increase of 6.21 km² coverage), potentially as a result of successional transitions from Cocos Bon-Dieu. The degree to which these changes are attributable to methodological differences between maps made from air photo interpretation and satellite image classification is unclear.
3. Bathymetric change modeling in the lagoon indicates removal of a net volume of 0.55 km³ of sediment, which has likely had important implications for hydrodynamic flow across the lagoon basins.
4. A synoptic habitat map of the benthic character of the lagoon and outer forereef atoll areas is presented as a baseline record of the marine environment.

Several clear management implications follow on from these findings. The value of an ongoing program to quantitatively measure shoreline change consistently at a representative set of sites around the atoll rim is highlighted. Such a program would enable the nature of long-term sediment dynamics to be ascertained at the atoll scale. Given the location and magnitude of changes to the lagoon bathymetry as a result of dredging activities, it would be pertinent to also monitor changes in water flow between the ocean and lagoon basin. This would focus on how flow speeds influence lagoon benthic ecology and also examine potential increases in sediment export from the lagoon sink. In view of the fact

that the benthic habitat map presented here is the first detailed synoptic record of the benthic character around Diego Garcia atoll, it is suggested that an ongoing program is established to map periodic changes in this character, particularly in view of the aforementioned climate related drivers of change.

This appraisal of ecological and geomorphic change has resulted in several findings of relevance to similar studies of oceanic atolls. The variability in shoreline change around the atoll rim across the assessment period highlights the distinction between different “narrow” and “normal” rim segments. This suggests that it may be an oversimplification to treat atolls as a single unit for the purpose of change assessments and future studies may profit from subdividing atoll structures into areas that relate to local environmental regimes before quantifying change. It is also worth regarding apparent changes observed through the comparison of maps produced at different time periods with caution. Changes may be attributable to methodological differences in map production. This is particularly the case with atoll environments, which have long been the focus of military interest due to their provision of a remote, sheltered environment in a central oceanic location from which numerous countries may be accessed. This interest has given rise to considerable archives of historical air photography and associated map products that provide a useful baseline against which change assessments can be made. When employing this baseline information, it is prudent to be aware of the important differences (e.g., in resolution, spatial referencing techniques, detail incorporated) between historical datasets and those derived from more recently available airborne and satellite remote sensing datasets.

Acknowledgments

This work would not have been possible without the donation of three IKONOS satellite images from the GeoEye Foundation (SH) and a research fellowship grant from The BLUE Marine Foundation (HE). Valuable field datasets were provided by Bernhard Riegl and Sam Purkis of the National Coral Reef Institute (ground referencing points in the northern section of the atoll lagoon) and Charles Sheppard, University of Warwick (georeferenced photorecords of seawater inundations around the atoll rim). Tom Spencer, University of Cambridge, is thanked for assistance with geospatial interpretation.

References

1. Sheppard, C.R.C.; Ateweberhan, M.; Bowen, B.W.; Carr, P.; Chen, C.A.; Clubbe, C.; Craig, M.T.; Ebinghaus, R.; Eble, J.; Fitzsimmons, N.; *et al.* Reefs and islands of the Chagos Archipelago, Indian Ocean: Why it is the world’s largest no-take marine protected area. *Aquat. Conserv. Mar. Freshw. Ecosyst.* **2012**, *22*, 232–261.
2. Sheppard, C.R.C. Corals of Chagos, and the role of Chagos reefs in the Indian Ocean. In *Ecology of the Chagos Archipelago*; Sheppard, C.R.C., Seaward, M.R.D., Eds.; Linnean Society/Westbury Publishing: London, UK, 1999; pp. 53–66.
3. Schott, F.; McCreary, J.P. The monsoon circulation of the Indian Ocean. *Prog. Oceanogr.* **2001**, *51*, 1–123.
4. Stoddart, D.W. Geology and Morphology of Reefs: Environment and History in Indian Ocean Reef Morphology. In *Regional Variation in Indian Ocean Coral Reefs*; Stoddart, D.W., Yonge, M., Eds.; Zoological Society of London Symposia 28; Academic Press: London, UK, 1971; pp. 3–31.

5. Pirazzoli, P.A. *World Atlas of Holocene Sea-Level Changes (Elsevier Oceanography Series)*; Elsevier: Amsterdam, Netherland, 1991.
6. Kench, P.S.; McLean, R.F.; Nichol, S.L. New model of reef-island evolution: Maldives, Indian Ocean. *Geology* **2005**, *33*, 145–148.
7. Blair, A. *Remarks and Observations in a Survey of the Chagos Archipelago, by Lieutenant Archibald Blair, 1786 and 1787. Published from the MSS at the Charge of the East India Company, by A. Dalrymple. 1788*, 1st ed.; George Biggs: London, UK, 1788.
8. Sheppard, C.R.C.; Spalding, M.; Bradshaw, C.; Wilson, S. Erosion vs. Recovery of coral reefs after 1998 El Niño: Chagos reefs, Indian Ocean. *Ambio* **2002**, *31*, 40–48.
9. Sheppard, C.R.C.; Dixon, D.J.; Gourlay, M.; Sheppard, A.L.S.; Payet, R. Coral mortality increases wave energy reaching shores protected by reef flats: Examples from the Seychelles. *Estuar. Coast. Shelf Sci.* **2005**, *64*, 223–234.
10. Mumby, P.J.; Skirving, W.; Strong, A.E.; Hardy, J.T.; LeDrew, E.F.; Hochberg, E.J.; Stumpf, R.P.; David, L.T. Remote sensing of coral reefs and their physical environment. *Mar. Pollut. Bull.* **2004**, *48*, 219–228.
11. Phinn, S.R.; Roelfsema, C.M.; Stumpf, R. Remote Sensing: Discerning the Promise from the Reality. In *Integrating and Applying Science: A Handbook for Effective Coastal Ecosystem Assessment*; Longstaff, B.J., Carruthers, T.J.B., Dennison, W.C., Lookingbill, T.R., Hawkey, J.M., Thomas, J.E., Wicks, E.C., Woerner, J., Eds.; IAN Press: Maryland, MD USA, 2010; pp. 201–222.
12. Stoddart, D.R. Geomorphology of Diego Garcia Atoll. *Atoll Res. Bull.* **1971**, *194*, 7–26.
13. Whistler, W.A. *Botanical Survey of Diego Garcia, Chagos Archipelago, British Indian Ocean Territory. NRMP Diego Garcia*; ISLE Botanica: Honolulu, HI, USA, 1996. Available online: <http://www.zianet.com/tedmorris/dg/2005NRMP-Appendix-botanicalsurvey.pdf> (accessed on 27 July 2012).
14. Kench, P.S.; Brander, R.W. Wave processes on coral reef flats: Implications for reef geomorphology using Australian case studies. *J. Coastal Res.* **2006**, *22*, 209–223.
15. Ford, M. Shoreline changes on an Urban Atoll in the Central Pacific Ocean: Majuro Atoll, Marshall Islands. *J. Coastal Res.* **2012**, *28*, 11–22.
16. Sheppard, C.R.C. Personal Communication. University of Warwick, Coventry, UK, 2012.
17. Mather, P.M. *Computer-Processing of Remotely-Sensed Images*; John Wiley and Sons: Chichester, UK, 2004.
18. Xie, Y.; Peng, M. Monitoring land use change using remote sensing and GIS. *Proc. SPIE* **2008**, doi: 10.1117/12.815747.
19. Lyzenga, D.R. Remote sensing of bottom reflectance and water attenuation parameters in shallow water using aircraft and Landsat data. *Int. J. Remote Sens.* **1981**, *2*, 71–82.
20. Hamylton, S. An evaluation of waveband pairs for water column correction using band ratio methods for seabed mapping in the Seychelles. *Int. J. Remote Sens.* **2011**, *32*, 9185–9195.
21. Purkis, S.J.; Graham, N.A.J.; Riegl, B.M. Predictability of reef fish diversity and abundance using remote sensing data in Diego Garcia (Chagos Archipelago). *Coral Reef.* **2008**, *27*, 167–178.
22. Congalton, R.G. A review of assessing the accuracy of classifications of remotely sensed data. *Remote Sens. Environ.* **1991**, *37*, 35–46.

23. Smithers, S.; Hopley, D. Coral Cay Classification and Evolution. In *Encyclopedia of Modern Coral Reefs: Structure, Form and Process*; Hopley, D., Ed.; Springer: Berlin, Germany, 2011; pp. 237–253.
24. Woodroffe, C.D. Reef-island topography and the vulnerability of atolls to sea-level rise. *Global Planet. Change* **2008**, *62*, 77–96.
25. Hamylton, S.; Spencer, T. Geomorphological modeling of tropical marine landscapes: Optical remote sensing, patches and spatial statistics. *Cont. Shelf Res.* **2011**, *31*, 151–161.
26. Woodroffe, C.D.; McLean, R.; Smithers, S.; Lawson, E. Atoll reef-island formation and response to sea-level change: West Island, Cocos (Keeling) Islands. *Mar. Geol.* **1999**, *160*, 85–104.
27. Sheppard, C.R.C. The coral fauna of Diego Garcia lagoon following harbour construction. *Mar. Pollut. Bull.* **1980**, *11*, 227–230.
28. Hamylton, S.; Spencer, T.; Hagan, A. Spatial modelling of benthic cover using remote sensing data in the Aldabra lagoon, Western Indian Ocean. *Mar. Ecol. Progr.* **2012**, *460*, 35–47.
29. Brock, V.E.; Van Heukelem, W.; Helfrich, P. *An Ecological Reconnaissance of Johnston Island and the Effects of Dredging*; University of Hawaii, Hawaii Institute of Marine Biology: Honolulu, HI, USA, 1966; Volume 11, pp. 1–56.
30. Ristvet, B.L.; Tremba, E.L.; Couch, R.F.; Fetzer, J.A.; Goter, E.R.; Walter, D.F.; Wendland, V.P. *Geological and Geophysical Investigations of the Eniwetok Nuclear Craters*; US Air Force Weapons Laboratory, Kirtland AFB: Albuquerque, NM, USA, 1978.
31. Noshkin, V.E.; Robison, W.L.; Wong, K.M.; Brunk, J.L.; Eagle, R.J.; Jones, H.E. Past and present levels of some radionuclides in fish from Bikini and Enewetak atolls. *Health Phys.* **1997**, *73*, 49–65.